Acoustics'08 Paris
June 29-July 4, 2008
www.acoustics08-paris.org

Acoustic radiation of low frequency flexural vibration modes in a submerged plate

Dominique Decultot[a], Romain Liétard[a], Farid Chati[a], Gerard Maze[b] and Aleksander Klauson[c]

[a]LOMC FRE 3102 CNRS Groupes Ondes Acoustiques, Université du Havre (IUT), Place Robert Schuman, 76610 Le Havre, France
[b]LAUE, Université du Havre, Place Robert Schuman, F-76610 Le Havre, France
[c]Tallinn University of Technology, Dept. of Mechanics, Ehitajate tee 5, 19086 Tallinn, Estonia
gerard.maze@univ-lehavre.fr

In some submarine structures, the acoustic structure-borne radiation at the neighbourhood of sonar equipments limits their use. So the aim of this study is to understand the process of acoustic radiation of a submerged plate subjected to a vibration. For the low frequency domain, only two types of wave can propagate: the first antisymmetric Lamb wave ($\boldsymbol{A_0}$) and the first symmetric Lamb wave ($\boldsymbol{S_0}$). When the plate is immersed in water the $\boldsymbol{A_0}$ wave is modified and the new wave is named $\boldsymbol{A}$ wave. In this work, experimental and numerical analysis of vibration modes in a plate are carried out. The studied rectangular plate of thickness 10 mm is made of steel. Its length and width are respectively 1.0 m and 0.5 m. The plate is partially immersed in water (90%). Flexural vibrations are generated by a shaker normally connected to the emerging plate part. The applied signal has one sinusoidal period at a frequency which is much lower than the critical frequency. Relations between vibration modes on the limited plate, admittances of the plate and the radiated pressure in water are highlighted.

1 Introduction

In order to reduce the radiation of plate in surrounding fluid, it is necessary to know better the relation between the vibration and the radiated acoustic pressure. For a plate in vacuum, two low frequency waves can propagate: the first antisymmetric Lamb wave $\boldsymbol{A_0}$ (flexural wave) and the first symmetric Lamb wave $\boldsymbol{S_0}$ (compressional wave) [1-2]. When the plate is immersed in water, the phase velocity of the flexural wave is modified and the new wave is named $\boldsymbol{A}$ or in case of cylindrical shell $\boldsymbol{A_0^-}$ wave [3]. Its phase velocity is always subsonic. When the frequency increases an other solution appears which corresponds to the $\boldsymbol{A_0}$ wave in vacuum. The $\boldsymbol{A}$ wave phase velocity tends to the sound velocity in water and the $\boldsymbol{A_0}$ wave phase velocity tends to Rayleigh wave velocity. In our work the studied frequencies are under the critical frequency.

The aim of this work is to identify the wave that propagates in a plate and which may radiate in water. The identification of this wave is achieved by identification of vibration mode in a finite plate [4]. These vibration modes are related to the number of half wavelengths extended on the two dimensions of the plate and also to the bending wave phase velocity. Relations between (i) these vibration modes established in the limited dimensions of the plate, (ii) the nature of the propagating wave, (iii) admittances of the plate and (iiii) the radiated pressure are highlighted. The comparison of the experimental results to well known analytical as well as numerical results helps to understand the radiated acoustic process of a normally excited partly submerged plate.

2 Experimental set-ups

The studied plate is made of steel with a thickness h = 10 mm. Its length and width are respectively L_y = 1.0 m and L_x = 0.5 m. The plate is partially immersed in water (90%). Two experimental set-ups are used in this study: one for the acoustic pressure measurements and another to the vibration measurements. In the two cases, the plate excitation process is the same and is described on figures 1 and 2. A shaker Brüel & Kjær 4809 is connected to the plate by means of a steel stinger. A signal composed of one sinusoidal period is applied to the shaker via a power amplifier Brüel & Kjær 2718. The mechanical pulse is transmitted to the plate by the steel stinger and a force transducer Brüel & Kjær 8230. The excitation of the plate is normally applied to the emerged plate part in order to generate flexural mode.

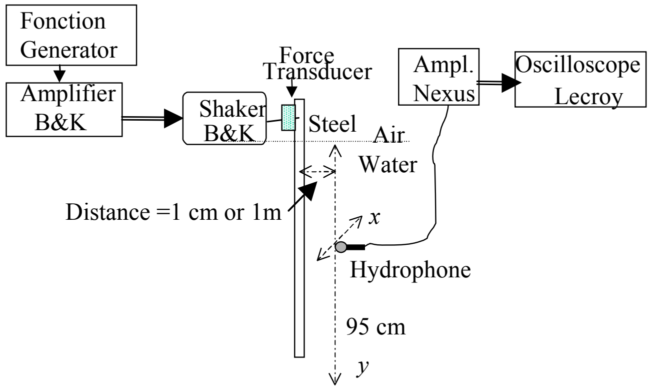

Fig.1 Experimental set-up of the acoustic pressure measurements.

The measurement of the pressure radiated by the submerged plate part (Fig. 1) is achieved by a hydrophone Brüel & Kjær 8105. The received signal is amplified by an amplifier Brüel & Kjær Nexus and is recorded in an oscilloscope Lecroy. The distance between the hydrophone and the plate is 10 mm or 1 m. With an appropriate system, the hydrophone moves along the plate in two directions (x, y).

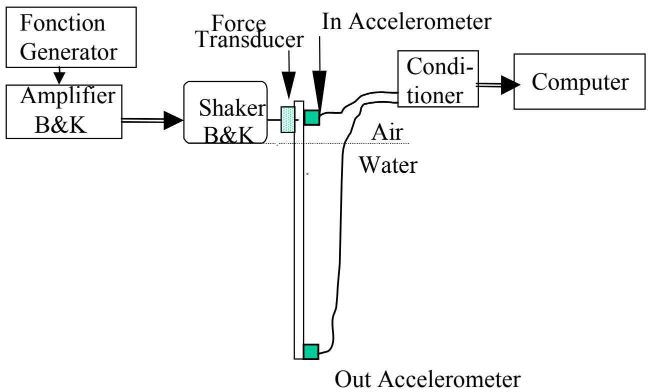

Fig. 2 Experimental set-up of vibration measurements.

The measurement of vibrations of the plate are achieved with two accelerometers PCB 352 mounted on two points on the plate (Fig. 2) and measuring the normal displacements. Figure 3 shows the dimensions of the studied plate with a front view. The hatched part corresponds to the scanned area used to identify the vibration mode. The two cross points indicate the position of the two accelerometers used to measure normal displacements. One is mounted in front of the connection between the shaker and the plate (impact point). It's labelled *driving point* or *in point*. The second accelerometer is mounted on the bottom of the plate and is labelled *out point.*

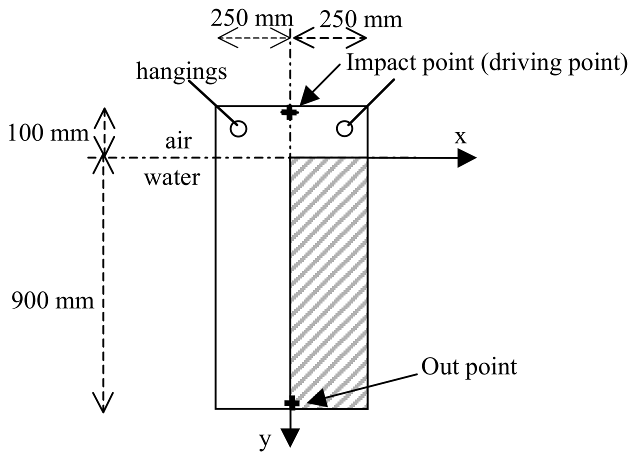

Fig. 3 Plate dimensions; hatched part is the scanned area for identification of vibration mode; cross points correspond to the position of accelerometers (driving point and out point).

3 Vibration mode study

3.1 Vibration mode identification

To identify the vibration modes and their corresponding frequencies, we used the set-up described on figure 1 where the distance between the hydrophone and the plate is 10 mm. The measurement is achieved by the hydrophone for different positions highlighting nodes and antinodes of pressure on scan image. When a resonance is appeared an integer number of half wavelengths has set up on each dimension of the plate. Figure 4 presents results of acoustic intensity over the force transmitted from the shaker to the plate. Spectra are calculated from measurements for hydrophone position $x = 0$ (central axis of the plate) and for different y positions: from 0 mm (air/water interface) to 950 mm (50 mm under plate edge). On the figure 4, only vibration modes with an antinode on y-axis can be observed. These vibration modes present an even number of half wavelengths on the width of the plate.

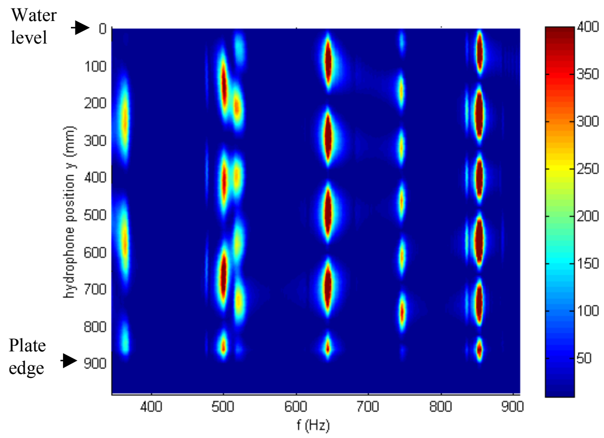

Fig.4 Acoustic Intensity / Force spectra for hydrophone position at the central axis x= 0 (linear scale).

In order to identify vibration modes for isolate frequencies on figure 4, the scanning of the plate is performed on the area hatched on the figure 3 (0<x (mm) <300 and 0<y (mm) <950). Figures 5 and 7 present results of these scans for respectively f = 517 Hz and f = 650 Hz. Finite element modelling of the partly submerged plate is made using ANSYS code. The corresponding numerical results are presented on figure 6 and figure 8 for respectively 510 Hz and 645 Hz. Identifications are achieved by counting the number of antinodes of vibration in the length and in the width of the plate. On figures 5 and 6, the mode (6, 0), which corresponds to six half wavelengths (n_y = 6) in the total length of the plate (1000 mm) and to zero half wavelength in the width of the plate (and n_x = 0) is identified. In the same way, figures 7 and 8 present the mode (5, 2) identification for the frequency 650 Hz and 645 Hz where n_y =5 and n_x = 2. Pressure plotted on figures 4-8 shows that there is no wave radiation for the given frequency range. On figures 4-8 no pressure is measured beyond the plate edges. Other identifications are achieved and their results are used to identify the wave type which propagates on the plate [4].

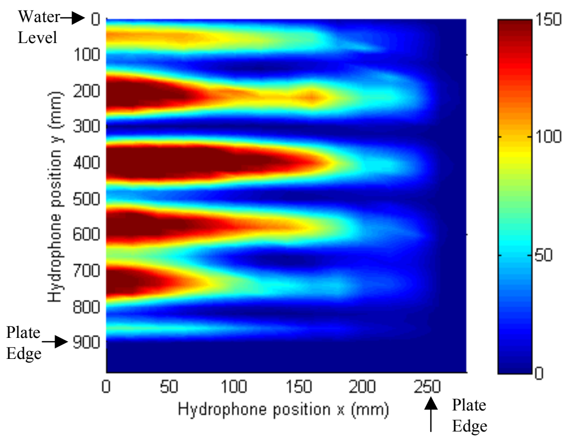

Fig.5 Experimental identification of the mode 6,0 (linear scale); n_y = 6, n_x= 0, f = 517 Hz.

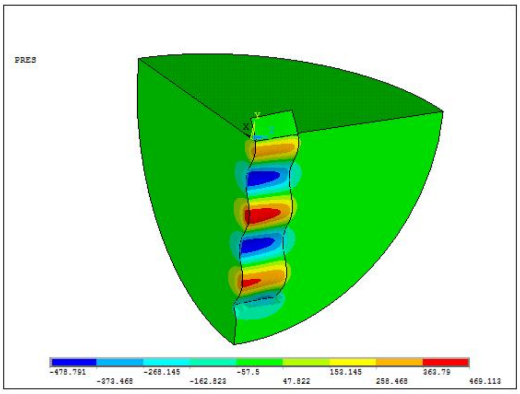

Fig.6 Numerical identification of the mode 6,0; $n_y = 6$, n_x=0, f = 510 Hz.

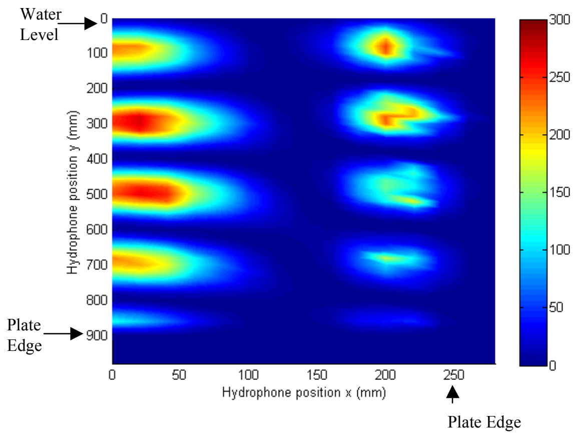

Fig.7 Experimental identification of the mode 5,2; $n_y = 5$, n_x= 2, f = 650 Hz.

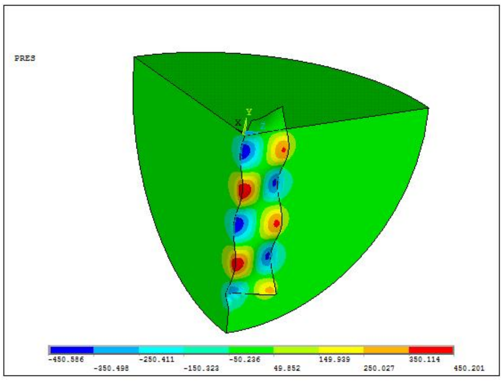

Fig. 8 Numerical identification of the mode 5,2; n_y=5, n_x=2, f = 645 Hz.

3.2 Wave type identification

The plate is attached by means of two slings. Free-free boundary conditions are considered in our experimental conditions and are validated by identification on figures 5 - 8. Antinodes are observed at the plate edges. If we consider vibration modes with node lines parallel to main plate axis, vibration modes occur when an integer number (n_y, n_x) of half wavelengths ($\lambda_y/2$, $\lambda_x/2$) has set up in the two dimensions (L_y, L_x) of the plate respectively:

$$n_y = \frac{2L_y}{\lambda_y} \quad \text{and} \quad n_x = \frac{2L_x}{\lambda_x}. \tag{1}$$

The wave number can be written as:

$$k^2 = k_x^2 + k_y^2 \tag{2}$$

and the wave phase velocity can be calculated from this expression:

$$C = \frac{2 f_{n_x n_y}}{\sqrt{\dfrac{n_x^2}{L_x^2} + \dfrac{n_y^2}{L_y^2}}}. \tag{3}$$

Where $f_{n_x n_y}$ is the measured frequency of the identified vibration mode (n_x, n_y). The phase velocity is calculated for identified vibration modes and is reported on figure 9 as diamond points.

In order to identify the wave which is at the origin of this vibration mode the calculation of the phase velocity of the flexural wave is achieved from the characteristic equation Eq. (4) [1]:

$$\begin{aligned}&(k^2+s^2)^2 sh(qd)ch(sd) - 4k^2 qs\, sh(sd)ch(qd)\\ &+\frac{\rho_W}{\rho_p}\frac{C_w^2}{C_t^2}\frac{q}{r}\left(k^2-s^2\right)\left(k^2-r^2\right)ch(qd)ch(sd)=0\end{aligned} \tag{4}$$

where $q^2 = k^2 - k_\ell^2$; $s^2 = k^2 - k_t^2$; $r^2 = k^2 - k_w^2$. $k = \dfrac{2\pi f}{C}$, $k_t = \dfrac{2\pi f}{C_t}$, $k_\ell = \dfrac{2\pi f}{C_\ell}$ and $k_w = \dfrac{2\pi f}{C_w}$ are the wave numbers, where C_ℓ and C_t are respectively the longitudinal and shear wave velocities in the plate (C_ℓ= 5790 m/s and C_t= 3100 m/s for steel); C_w is sound velocity in water (C_w= 1470 m/s); d is the plate half thickness; ρ_p and ρ_w are respectively the mass density of the plate and of the fluid medium (ρ_p = 7900 kg/m^3 and ρ_w = 1000 kg/m^3).

The resolution of the equation Eq. 4 is achieved for two cases: (i) in the vacuum with ρ_w = 0 the result is presented on figure 9 by a upper solid line; (ii) with water as fluid medium so that ρ_w =1000 kg/m^3 in this case the result is presented as a lower solid line on figure 9. In the case of vacuum, the limit for high frequencies is the Rayleigh wave velocity: this solution corresponds to the $\boldsymbol{A_0}$ flexural wave. With the presence of water as fluid medium the lower limit for high frequencies of the phase velocity is the sound velocity in water. So this wave has the characteristics of the $\boldsymbol{A}$ wave. The solutions of this $\boldsymbol{A}$ wave coincide with results obtained from experimental vibration mode identifications and calculated with Eq. 3. So the wave propagating in the immersed part of the plate is the $\boldsymbol{A}$ wave. The imaginary part of the $\boldsymbol{A}$ wave root is equal to zero for the studied frequency band. In this case the wave does not radiate in the fluid medium. The pressure which is experimentally measured in very near field is due to the vibration when the $\boldsymbol{A}$ wave is propagating on the plate. No pressure radiation is detected at the edges of plate (figures 4-8).

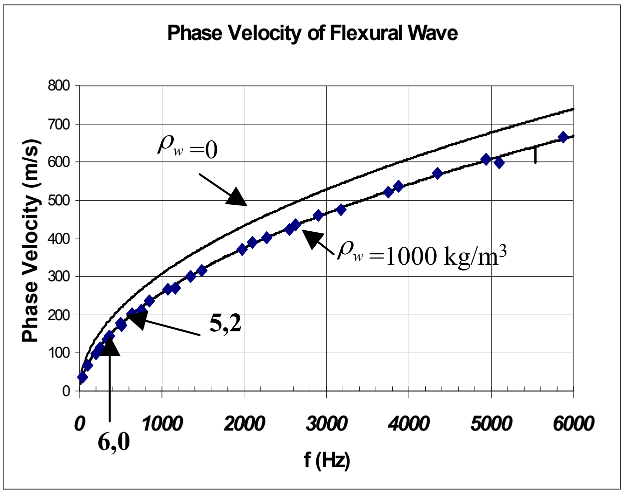

Fig. 9 Phase velocity of the flexural wave; upper solid curve: calculation with ρ_w =0; lower solid curve: calculation with ρ_w =1000 kg/m^3;♦: vibration modes and frequencies experimentally identified.

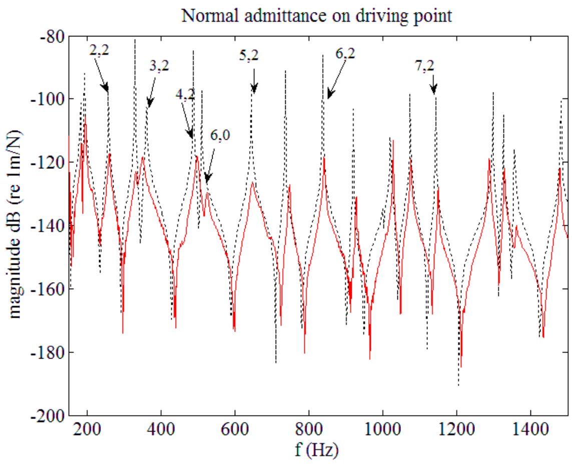

Fig.10 Normal admittance on the driving point: experimental results (solid curve); numerical results (dashed curve); numerical values n_x,n_y of vibration mode are indicated.

4 Mechanical measurements

4.1 Admittance results

The study of admittance is achieved with the set-up previously described on the figure 2. The accelerometer placed on the driving point measures the normal displacement in front of the impact point. The admittance is expressed here as the ratio of the displacement over the force transmitted by the shaker to the plate. On the figure 10, the admittance is represented for the frequency band 150 Hz to 1500 Hz. The solid curve is experimental result and the dashed curve is numerical result. There is a good agreement between these two results. The normal admittance presents maxima for frequencies which correspond to a vibration mode identified by the previous method described before. Some of the vibration modes are indicated on the figure with their numerical values n_x,n_y.

Admittance on the out point is realized by an another accelerometer placed as indicated on figures 2 and 3. The comparison between admittance on the driving point (also labeled Input admittance) and admittance on the out point is shown on the figure 11. Maxima of admittance occur at resonance frequencies. For these frequencies input admittance and output admittance are nearly equivalent, thus indicated good vibration transmission.

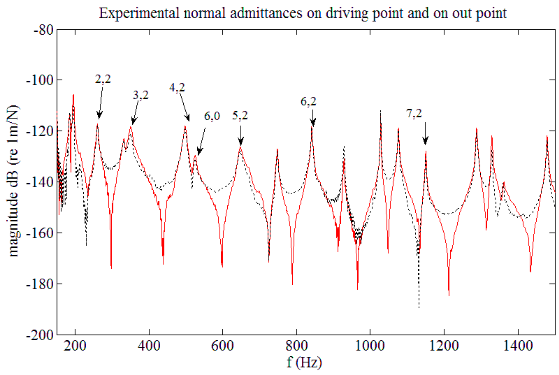

Fig. 11 Experimental normal admittances on driving point (solid curve) and on out point (dashed curve).

4.2 Radiated pressure

On the figure 12, the ratio pressure over the force is presented for the frequency band 150-1500 Hz. The pressure is measured with the set-up described on the figure 1. In this case the distance between the plate and the hydrophone is equal to 1 m. The hydrophone is situated on the central axis (x=0) and moves from the air/water interface to 950 mm under the water. The lobes of pressure are highlighted on result of the figure 12; they correspond to the resonance frequencies of the plate. These lobes are growing with the depth of the hydrophone. Figure 13 presents on the upper curve an extract of the figure 12 for the hydrophone position y= 400 mm. The lower curve presents the experimental admittance of the driving point (extract of figure 10). The maxima of radiated pressure and the maxima of admittance are observed for the same frequencies. Some corresponding identified vibration modes n_x,n_y are indicated on this figure. The pressure lobes are so large that vibration antinodes in the length of the plate cannot be distinguished anymore.

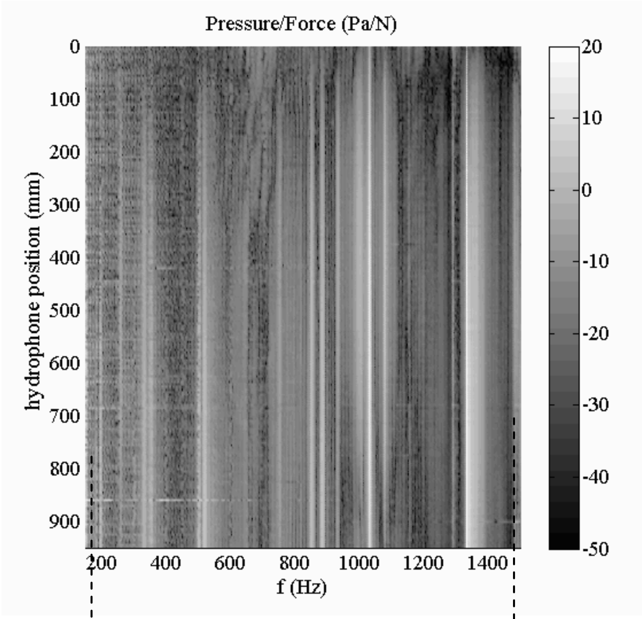

Fig. 12 Experimental radiated pressure of the plate.

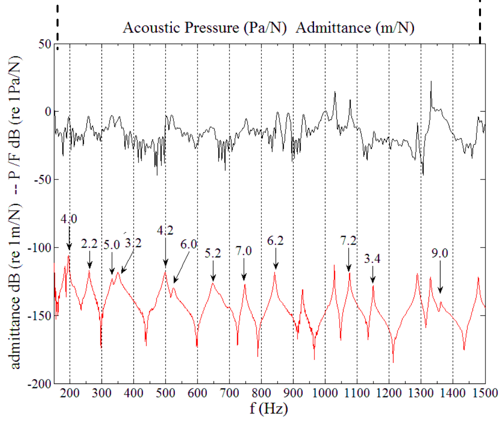

Fig. 13 Upper curve: experimental radiated pressure for hydrophone position y = 400 mm (extract of the figure 12). Lower curve: experimental normal admittance on the driving point.

The figure 14 presents the comparison between the numerical results (dashed curve) and experimental ones (solid curve). They are obtained in the same configuration positions and show a rather good agreement, although the peaks appear less damped in Finite Elements modelling than in measurements. Amplitude of maxima of radiated pressure depends on the angular diagram which also depends on the value of the vibration mode n_x,n_y [5].

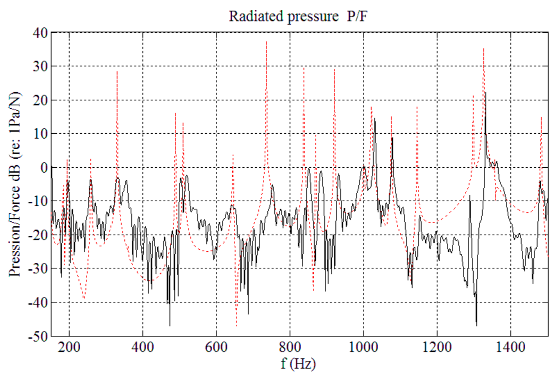

Fig. 14 Radiated pressure of the plate for the position of hydrophone = 1 m, x = 0 and y =400 mm. dashed curve: numerical results; solid curve: experimental results.

5 Conclusion

In this paper, the experimental set-up used to generate the subsonic flexural wave is described. The studied plate is partly immersed in water. Some identifications of vibration modes established in two dimensions of the limited plate allow us to determine the ***A*** wave propagating in the plate. For the studied frequency band, no pressure radiation is detected beyond the edges of the plate and only pressure due to the vibration of the plate is measured in very near field. The study of input and output admittances shows the behaviour of the plate for vibration mode frequencies. In these cases the plate transmitted all the vibration from the input point to the out point. Moreover maxima of radiated pressure are measured for the frequencies of vibration modes.

Acknowledgments

The authors are grateful for Michel Pompei of the Paulstra Vibrachoc Company for his scientific and financial support. The support of the Estonian Science Foundation (ETF) is gratefully acknowledged.

References

[1] A. Viktorov, “Rayleigh and Lamb Waves”, *Plenum Press*, New York, (1967).

[2] M. C. Junger, D. Feit, “Sound, Stuctures and Their Interaction”, *The MIT Press*, Cambridge, Massachusetts, London , England (1986).

[3] G. Maze, F. Léon, J. Ripoche, H. Überall, “Repulsion phenomena in the phase velocity dispersion curves of circumferential waves on elastic cylindrical shells”, *J. Acoust. Soc. Am.* 105, 1965-1701 (1999).

[4] Décultot Dominique, Chati Farid, Maze Gérard, Klauson Aleksander, “Experimental Identification of very low frequency flexural vibration modes of partly submerged plate”, *PHY-07-008* 19th ICA Madrid September 2007.

[5] L. Shuyu, “Study on the radiation acoustic field of rectangular radiators in flexural vibration”, *Journal of Sound and Vibration* 254(3), 469-479 (2002).